Moment equations for probability distributions in classical and quantum mechanics

L. E. Ballentine and S. M. McRae
Physics Department, Simon Fraser University, Burnaby, British Columbia, Canada V5A 1S6
(Received 27 January 1998)

The equations of motion for phase-space moments and correlations are derived systematically for quantum and classical dynamics, and are solved numerically for chaotic and regular motions of the Hénon-Heiles model. For very narrow probability distributions, Ehrenfest's theorem implies that the centroid of the quantum state will approximately follow a classical trajectory. But the error in Ehrenfest's theorem does not scale with $\hbar$, and is found to be governed essentially by classical quantities. The difference between the centroids of the quantum and classical probability distributions, and the difference between the variances of those distributions, scale as $\hbar^2$, and so are the true measures of quantum effects. For chaotic motions, these differences between quantum and classical motions grow exponentially, with a larger exponent than does the variance of the distributions. For regular motions, the variance of the distributions grows as t^2, whereas the differences between the quantum and classical motions grow as t^3. [S1050-2947(98)13009-3]

PACS number(s): 03.65.Sq, 03.20.+i, 05.45.+b

I. INTRODUCTION

In several areas of current research, such as mesoscopic quantum systems and quantum chaos, it is important to obtain a better understanding of the similarities and differences between classical and quantum dynamics, and of the emergence of classical behavior from quantum mechanics. Since the predictions of quantum theory are in the form of probabilities, it is appropriate to compare the dynamics of a quantum state with that of a classical statistical distribution, rather than with a single classical trajectory [1]. If the initial quantum state is chosen to be a small wave-packet, and the initial classical ensemble is chosen to match its position and momentum distributions, then we can distinguish three distinct dynamical regimes, as follows.

(a) The Ehrenfest regime, in which the widths of the quantum and classical probability distributions are small compared to the physical dimensions of the system. The centroid of the quantum state, and also that of the classical ensemble, approximately follow a classical trajectory (Ehrenfest's theorem).

(b) The widths of the quantum and classical distributions are comparable to the dimensions of the system. Ehrenfest's theorem does not apply, but the quantum and classical probability distributions are approximately equal.

(c) The fully quantum regime, characterized by interference and quantum recurrence, in which there is no correspondence between the classical and quantum probability distributions.

We have chosen to study the equations satisfied by the phase-space moments and correlations of quantum and classical systems for several reasons, as follows.

(i) In a numerical integration of the Schrödinger equation, it is impractical to use a dimensionless Planck constant (essentially the ratio of the de Broglie wavelength to the size of the system) that is much smaller than 10^{-3}. No such restriction applies to the moment equations.

(ii) The corrections to Ehrenfest's theorem involve moments of the probability distributions, hence their time evolution is of interest.

(iii) The moment equations offer another way to study the differences between the quantum dynamics of states whose classical motions are chaotic or regular.

The structure of the moment equations has been studied formally [2], but they have not previously been applied numerically. We shall find that the moment method works only in the Ehrenfest regime (a), but in that regime it yields some new and interesting results.

II. MOMENT EQUATIONS

The equations of motion for the average position and momentum of both classical and quantum probability distributions depend upon the higher moments of the distribution, creating, in general, an infinite hierarchy of equations to be solved. We shall study them for one- and two-dimensional systems.

A. One-dimensional quantum moment hierarchy

In this section, we will derive a hierarchy of moment equations that arises from corrections to Ehrenfest's theorem.

Assume a Hamiltonian operator of the form

$$\hat{H}=\frac{\hat{p}^2}{2}+V(\hat{q}). \tag{1}$$

We are interested in the time development of the average position and average momentum. The equations can be derived by using the time dependent Schrödinger equation and integrating by parts (as Ehrenfest did in his 1927 paper [3]), but it is easier to start from the Heisenberg equations of motion:

$$\frac{d\hat{q}}{dt}=\frac{i}{\hbar}[\hat{H},\hat{q}]=\hat{p}, \tag{2}$$

$$\frac{d\hat{p}}{dt}=\frac{i}{\hbar}[\hat{H},\hat{p}]=-\frac{dV(\hat{q})}{d\hat{q}}. \tag{3}$$

Taking the average in some initial state yields

$$\frac{d}{dt}\langle\hat{q}\rangle=\langle\hat{p}\rangle, \tag{4}$$

$$\frac{d}{dt}\langle\hat{p}\rangle=-\left\langle\frac{dV(\hat{q})}{d\hat{q}}\right\rangle. \tag{5}$$

Let us define the mean position and momentum,

$$Q=\langle\hat{q}\rangle,\quad P=\langle\hat{p}\rangle, \tag{6}$$

and the operators for the deviations from the means,

$$\delta\hat{q}=\hat{q}-Q,\quad \delta\hat{p}=\hat{p}-P. \tag{7}$$

The Hamiltonian operator and the time evolution equations can be written in terms of these new quantities as

$$\hat{H}=\frac{(\delta\hat{p})^2}{2}+P(\delta\hat{p})+\frac{P^2}{2}+\sum_{l=0}^{\infty}\frac{d^lV(Q)}{dQ^l}\frac{(\delta\hat{q})^l}{l!}, \tag{8}$$

$$\frac{dQ}{dt}=P, \tag{9}$$

$$\frac{dP}{dt}=-\sum_{l=0}^{\infty}\frac{\langle(\delta\hat{q})^l\rangle}{l!}\frac{d^{l+1}V(Q)}{dQ^{l+1}}. \tag{10}$$

If the terms in Eq. (10) with $l>0$ could be neglected, then the quantum averages, Q and P, would satisfy the classical equations of motion. But, in fact, the time dependence of P depends, not only on the mean, but also on the higher moments of the position distribution, $\langle(\delta\hat{q})^l\rangle$. The resulting difference between the time development of the mean position Q and the classical orbit constitutes the error that would be committed by applying Ehrenfest's theorem.

Not only are the higher moments of the position distribution involved in the time development of P, but the time development of $\langle(\delta\hat{q})^l\rangle$ involves more complicated moments of the form $\langle(\delta\hat{p})^k(\delta\hat{p})^n\rangle$.

From Heisenberg's equations of motion we have

$$\frac{d}{dt}[(\delta\hat{p})^k(\delta\hat{q})^n]=\frac{i}{\hbar}[\hat{H},(\delta\hat{p})^k(\delta\hat{q})^n]+\frac{\partial}{\partial t}[(\delta\hat{p})^k(\delta\hat{q})^n], \tag{11}$$

where the final term involving $\partial/\partial t$ accounts for the explicit time dependence of Q and P in Eq. (7). The required commutator relationships can be calculated using Eq. (A1) from the Appendix. The final result is

$$\frac{d}{dt}\langle(\delta\hat{p})^k(\delta\hat{q})^n\rangle=n\langle(\delta\hat{p})^{k+1}(\delta\hat{q})^{n-1}\rangle+k\langle(\delta\hat{p})^{k-1}(\delta\hat{q})^n\rangle\sum_{l=0}^{\infty}\frac{\langle(\delta\hat{q})^l\rangle}{l!}\frac{d^{l+1}V(Q)}{dQ^{l+1}}-k\sum_{l=0}^{\infty}\frac{d^{l+1}V(Q)}{dQ^{l+1}}\frac{\langle(\delta\hat{p})^{k-1}(\delta\hat{q})^{n+l}\rangle}{l!}$$
$$+\frac{i\hbar n(n-1)}{2}\langle(\delta\hat{p})^k(\delta\hat{q})^{n-2}\rangle-k!\sum_{l=1}^{\infty}\frac{d^{l+1}V(Q)}{dQ^{l+1}}\sum_{s=2}^{\min(l+1,k)}\frac{(i\hbar)^{s-1}}{s!(l+1-s)!(k-s)!}\langle(\delta\hat{p})^{k-s}(\delta\hat{q})^{l+1-s+n}\rangle. \tag{12}$$

Similarly, using Eq. (A2), we find that

$$\frac{d}{dt}\langle(\delta\hat{q})^n(\delta\hat{p})^k\rangle=n\langle(\delta\hat{q})^{n-1}(\delta\hat{p})^{k+1}\rangle+k\langle(\delta\hat{q})^n(\delta\hat{p})^{k-1}\rangle\sum_{l=0}^{\infty}\frac{\langle(\delta\hat{q})^l\rangle}{l!}\frac{d^{l+1}V(Q)}{dQ^{l+1}}-k\sum_{l=0}^{\infty}\frac{d^{l+1}V(Q)}{dQ^{l+1}}\frac{\langle(\delta\hat{q})^{n+l}(\delta\hat{p})^{k-1}\rangle}{l!}$$
$$-\frac{i\hbar n(n-1)}{2}\langle(\delta\hat{q})^{n-2}(\delta\hat{p})^k\rangle-k!\sum_{l=1}^{\infty}\frac{d^{l+1}V(Q)}{dQ^{l+1}}\sum_{s=2}^{\min(l+1,k)}\frac{(-i\hbar)^{s-1}}{s!(l+1-s)!(k-s)!}\langle(\delta\hat{q})^{l+1-s+n}(\delta\hat{p})^{k-s}\rangle. \tag{13}$$

Using Eq. (A3), we can obtain a set of equations for the symmetrized operator products, which are the quantum moments:

$$\frac{d}{dt}\langle \tfrac{1}{2}[(\delta\hat{p})^k,(\delta\hat{q})^n]_+\rangle = n\langle \tfrac{1}{2}[(\delta\hat{p})^{k+1},(\delta\hat{q})^{n-1}]_+\rangle + k\langle \tfrac{1}{2}[(\delta\hat{p})^{k-1},(\delta\hat{q})^{n}]_+\rangle \sum_{l=0}^{\infty}\frac{\langle(\delta\hat{q})^l\rangle}{l!}\frac{d^{l+1}V(Q)}{dQ^{l+1}}$$

$$-k\sum_{l=0}^{\infty}\frac{d^{l+1}V(Q)}{dQ^{l+1}}\frac{1}{l!}\langle \tfrac{1}{2}[(\delta\hat{p})^{k-1},(\delta\hat{q})^{n+l}]_+\rangle$$

$$+\frac{n!k!}{2}\sum_{l=1}^{\min([(n-1)/2],[(k+1)/2])}\frac{(-1)^l\hbar^{2l}E_{2l-1}(0)}{(2l-1)!(n-2l-1)!(k-2l+1)!}\langle \tfrac{1}{2}[(\delta\hat{p})^{k-2l+1},(\delta\hat{q})^{n-2l-1}]_-+\rangle$$

$$-k!\sum_{l=1}^{\infty}\frac{d^{l+1}V(Q)}{dQ^{l+1}}\Bigg\{\sum_{j=1}^{[\min(l/2,(k-1)/2)]}\frac{(-1)^j\hbar^{2j}\left\langle\frac{1}{2}[(\delta\hat{p})^{k-2j-1},(\delta\hat{q})^{n+l-2j}]_+\right\rangle}{(k-2j-1)!(2j+1)!(l-2j)!}$$

$$+\sum_{j=1}^{[\min((l+n)/2,(k-1)/2)]}\frac{(-1)^j\hbar^{2j}\left\langle\frac{1}{2}[(\delta\hat{p})^{k-2j-1},(\delta\hat{q})^{n+l-2j}]_+\right\rangle}{(k-2j-1)!(l+n-2j)!}$$

$$\times\sum_{s=1}^{j}\frac{(l+n-2s+1)!E_{2j-2s+1}(0)}{(2s)!(l-2s+1)!(2j-2s+1)!}\Bigg\}. \tag{14}$$

Here the anticommutator, $[\hat{A},\hat{B}]_+=\hat{A}\hat{B}+\hat{B}\hat{A}$, is the symmetrized operator product. In the limits of the sums, $[x]$ indicates the integer part of x. $E_n(0)$ is the zeroth order coefficient of the nth Euler polynomial (see Abramowitz and Stegun [4], p. 809).

B. One-dimensional classical moment hierarchy

Ballentine, Yang, and Zibin [1] have pointed out that a classical analog of Ehrenfest's theorem can be obtained by considering a classical ensemble of noninteracting particles. The usual method of derivation is to let $\rho(q,p,t)$ be the probability distribution in phase space for a classical ensemble, which satisfies the Louiville equation,

$$\frac{\partial}{\partial t}\rho(q,p,t)=-p\frac{\partial}{\partial q}\rho(q,p,t)+\frac{dV(q)}{dq}\frac{\partial}{\partial p}\rho(q,p,t). \tag{15}$$

The classical average of a function $f(q,p)$ is defined as

$$\langle f(q,p)\rangle_c=\int_{-\infty}^{\infty}\int_{-\infty}^{\infty}f(q,p)\rho(q,p,t)dqdp. \tag{16}$$

This approach is analogous to using the Schrödinger picture in quantum mechanics, in which the time dependence is carried by the state function. Instead, we use a derivation that is analogous to the Heisenberg equations of motion, in which the time dependence is carried by the variables q and p, and the probability distribution ρ is a distribution over initial states.

Consider a Hamiltonian of the form

$$H=\frac{p^2}{2}+V(q). \tag{17}$$

From Hamilton's equations of motion we have

$$\frac{dq}{dt}=p, \tag{18}$$

$$\frac{dp}{dt}=-\frac{dV(q)}{dq}. \tag{19}$$

For the initial position and momentum, q_0 and p_0, the solution of the above equations is of the form $q=q(q_0,p_0,t)$ and $p=p(p_0,q_0,t)$. Letting $\rho(q_0,p_0)$ be the initial probability distribution in phase space for an ensemble, we can define the following classical averages:

$$Q_c=\langle q\rangle_c=\int_{-\infty}^{\infty}\int_{-\infty}^{\infty}q(q_0,p_0,t)\rho(q_0,p_0)dq_0dp_0, \tag{20}$$

$$P_c=\langle p\rangle_c=\int_{-\infty}^{\infty}\int_{-\infty}^{\infty}p(q_0,p_0,t)\rho(q_0,p_0)dq_0dp_0. \tag{21}$$

Let $\delta q=q-Q_c$ and $\delta p=p-P_c$ be the deviations from the mean values. Taking the ensemble average of both sides of Eqs. (18) and (19) yields

$$\frac{dQ_c}{dt}=P_c, \tag{22}$$

$$\frac{dP_c}{dt}=-\left\langle\frac{dV(q)}{dq}\right\rangle_c=-\sum_{l=0}^{\infty}\frac{\langle(\delta q)^l\rangle_c}{l!}\frac{d^{l+1}V(Q_c)}{dQ_c^{l+1}}, \tag{23}$$

where we have expanded $V(q)$ in a Taylor series in δq about the centroid. Notice that the equation for dP_c/dt depends upon the moments $\langle(\delta q)^l\rangle_c$ for $l\geqslant 0$. In general, we need to

know all higher order moments of the distribution. Using Hamilton's equations of motion and Eqs. (22) and (23), we obtain

$$\frac{d}{dt}(\delta p)^k(\delta q)^n = n(\delta p)^k(\delta q)^{n-1}(P_c+\delta p) - k(\delta p)^{k-1}(\delta q)^n\frac{dV(q)}{dq} \tag{24}$$

$$- n(\delta p)^k(\delta q)^{n-1}P_c - k(\delta p)^{k-1}(\delta q)^n\frac{dP_c}{dt}. \tag{25}$$

By taking the average of both sides of this equation, we obtain a general formula for the time derivatives of all the moments of the classical distribution,

$$\begin{aligned}\frac{d}{dt}\langle(\delta p)^k(\delta q)^n\rangle_c &= n\langle(\delta p)^{k+1}(\delta q)^{n-1}\rangle_c \\ &+ k\langle(\delta p)^{k-1}(\delta q)^n\rangle_c\sum_{l=0}^{\infty}\frac{\langle(\delta q)^l\rangle_c}{l!}\frac{d^{l+1}V(Q_c)}{dQ_c^{l+1}} \\ &- k\sum_{l=0}^{\infty}\frac{\langle(\delta p)^{k-1}(\delta q)^{n+l}\rangle_c}{l!}\frac{d^{l+1}V(Q_c)}{dQ_c^{l+1}}.\end{aligned} \tag{26}$$

C. Differences between the quantum and classical moment equations

The first three terms in the quantum hierarchy of Eq. (14) have the same form as those in the classical hierarchy of Eq. (26), but the remaining terms in Eq. (14) are corrections involving $\hbar$. As we can see from Eq. (14), the first appearance of $\hbar$ occurs in the equation for $d/dt\langle(\delta\hat{p})^3\rangle$. That the difference between the classical and quantum equations occurs only in third and higher orders provides part of the explanation for the fact that the classical and quantum probability distributions agree quite well for modest time intervals.

We have defined the quantum moments as the expectation values of the symmetrized products of the operators. One could ask whether there might be some other ordering of the $\delta\hat{q}$ and $\delta\hat{p}$ operators that could be used to define quantum moments that would correspond more closely to their classical analogs, and for which the first occurrence of $\hbar$ in the moment equation hierarchy would be pushed to a higher order. Suppose, for example, that instead of using $\frac{1}{2}[(\delta\hat{p})^2,(\delta\hat{q})^l]_+$ for the quantum moment corresponding to $\langle(\delta p)^2(\delta q)^l\rangle$, we redefined that quantum moment to be

$$\frac{1}{3}[(\delta\hat{p})^2,(\delta\hat{q})^l]_+ + \frac{1}{3}\delta\hat{p}(\delta\hat{q})^l\delta\hat{p} - \frac{\hbar^2}{6}l(l-1)(\delta\hat{q})^{l-2}. \tag{27}$$

The classical limit of this moment would not be affected, and we would eliminate all $\hbar$ terms in the equation for $d/dt\langle(\delta\hat{p})^3\rangle$. But this *same* redefinition would *not* eliminate all occurrences of $\hbar$ in the expression for $d/dt\langle\frac{1}{2}[(\delta\hat{p})^3,\delta\hat{q}]_+\rangle$. Indeed, no matter what ordering of operators is used, there will remain a difference between the evolution equations for the classical and quantum moments. It is the noncommutativity of the $\delta\hat{q}$ and the $\delta\hat{p}$ operators that is the source of this difference, and hence is the source of the difference between classical and quantum mechanics.

D. Conservation of energy

By writing the averages of the classical and quantum Hamiltonians as

$$\langle H\rangle_c = \frac{1}{2}[\langle(\delta p)^2\rangle_c + P_c^2] + \sum_{l=0}^{\infty}\frac{\langle(\delta q)^l\rangle_c}{l!}\frac{d^lV(Q_c)}{dQ_c^l} \tag{28}$$

and

$$\langle\hat{H}\rangle = \frac{1}{2}[\langle(\delta\hat{p})^2\rangle + P^2] + \sum_{l=0}^{\infty}\frac{\langle(\delta\hat{q})^l\rangle}{l!}\frac{d^lV(Q)}{dQ^l}, \tag{29}$$

respectively, it follows directly from the moment hierarchies that $d/dt\langle H\rangle_c = 0$ and $d/dt\langle\hat{H}\rangle = 0$. The accuracy with which these formal identities are satisfied in a numerical computation can be used to test the accuracy of the numerical solutions.

E. Two-dimensional moment hierarchy

The hierarchy of moment equations can be generalized to higher dimensional systems. We will develop them for a system of two degrees of freedom, since that is the smallest dynamical system that can exhibit chaos.

For a classical Hamiltonian of the form

$$H = \frac{1}{2}(p_1^2+p_2^2) + V(q_1,q_2), \tag{30}$$

we have

$$\frac{dQ_{c\alpha}}{dt} = P_{c\alpha}, \quad \alpha = 1,2, \tag{31}$$

$$\frac{dP_{c\alpha}}{dt} = -\sum_{l=0}^{\infty}\sum_{j=0}^{l}\frac{\langle(\delta q_1)^{l-j}(\delta q_2)^j\rangle_c}{(l-j)!j!}\frac{\partial^{l+1}V(Q_{c1},Q_{c2})}{\partial Q_{c\alpha}\partial Q_{c1}^{l-j}\partial Q_{c2}^j}, \quad \alpha = 1,2, \tag{32}$$

and

$$\frac{d}{dt}\langle(\delta p_1)^{k_1}(\delta p_2)^{k_2}(\delta q_1)^{n_1}(\delta q_2)^{n_2}\rangle_c = n_1\langle(\delta p_1)^{k_1+1}(\delta p_2)^{k_2}(\delta q_1)^{n_1-1}(\delta q_2)^{n_2}\rangle_c + n_2\langle(\delta p_1)^{k_1}(\delta p_2)^{k_2+1}(\delta q_1)^{n_1}(\delta q_2)^{n_2-1}\rangle_c$$
$$-k_1\frac{dP_{c1}}{dt}\langle(\delta p_1)^{k_1-1}(\delta p_2)^{k_2}(\delta q_1)^{n_1}(\delta q_2)^{n_2}\rangle_c$$
$$-k_2\frac{dP_{c2}}{dt}\langle(\delta p_1)^{k_1}(\delta p_2)^{k_2-1}(\delta q_1)^{n_1}(\delta q_2)^{n_2}\rangle_c$$
$$-k_1\sum_{l=0}^{\infty}\sum_{j=0}^{l}\frac{\langle(\delta p_1)^{k_1-1}(\delta p_2)^{k_2}(\delta q_1)^{n_1+l-j}(\delta q_2)^{n_2+j}\rangle_c}{(l-j)!j!}\frac{\partial^{l+1}V(Q_{c1},Q_{c2})}{\partial Q_{c1}^{l-j+1}\partial Q_{c2}^{j}}$$
$$-k_2\sum_{l=0}^{\infty}\sum_{j=0}^{l}\frac{\langle(\delta p_1)^{k_1}(\delta p_2)^{k_2-1}(\delta q_1)^{n_1+l-j}(\delta q_2)^{n_2+j}\rangle_c}{(l-j)!j!}\frac{\partial^{l+1}V(Q_{c1},Q_{c2})}{\partial Q_{c1}^{l-j}\partial Q_{c2}^{j+1}}. \tag{33}$$

The subscript α labels the degrees of freedom.

The corresponding equations for a quantum Hamiltonian of the form

$$\hat{H}=\frac{1}{2}(\hat{p}_1^2+\hat{p}_2^2)+V(\hat{q}_1,\hat{q}_2) \tag{34}$$

are

$$\frac{dQ_\alpha}{dt}=P_\alpha, \quad \alpha=1,2, \tag{35}$$

$$\frac{dP_\alpha}{dt}=-\sum_{l=0}^{\infty}\sum_{j=0}^{l}\frac{\langle(\delta\hat{q}_1)^{l-j}(\delta\hat{q}_2)^{j}\rangle}{(l-j)!j!}\frac{\partial^{l+1}V(Q_1,Q_2)}{\partial Q_\alpha\partial Q_1^{l-j}\partial Q_2^{j}}, \quad \alpha=1,2, \tag{36}$$

and

$$\frac{d}{dt}\langle(\delta\hat{p}_1)^{k_1}(\delta\hat{p}_2)^{k_2}(\delta\hat{q}_1)^{n_1}(\delta\hat{q}_2)^{n_2}\rangle$$
$$=n_1\langle(\delta\hat{p}_1)^{k_1+1}(\delta\hat{p}_2)^{k_2}(\delta\hat{q}_1)^{n_1-1}(\delta\hat{q}_2)^{n_2}\rangle+n_2\langle(\delta\hat{p}_1)^{k_1}(\delta\hat{p}_2)^{k_2+1}(\delta\hat{q}_1)^{n_1}(\delta\hat{q}_2)^{n_2-1}\rangle$$
$$-k_1\frac{dP_1}{dt}\langle(\delta\hat{p}_1)^{k_1-1}(\delta\hat{p}_2)^{k_2}(\delta\hat{q}_1)^{n_1}(\delta\hat{q}_2)^{n_2}\rangle-k_2\frac{dP_2}{dt}\langle(\delta\hat{p}_1)^{k_1}(\delta\hat{p}_2)^{k_2-1}(\delta\hat{q}_1)^{n_1}(\delta\hat{q}_2)^{n_2}\rangle$$
$$+\frac{i\hbar n_1(n_1-1)}{2}\langle(\delta\hat{p}_1)^{k_1}(\delta\hat{p}_2)^{k_2}(\delta\hat{q}_1)^{n_1-2}(\delta\hat{q}_2)^{n_2}\rangle+\frac{i\hbar n_2(n_2-1)}{2}\langle(\delta\hat{p}_1)^{k_1}(\delta\hat{p}_2)^{k_2}(\delta\hat{q}_1)^{n_1}(\delta\hat{q}_2)^{n_2-2}\rangle$$
$$-k_1!\sum_{l=0}^{\infty}\sum_{j=0}^{l}\frac{1}{j!}\frac{\partial^{l+1}V(Q_1,Q_2)}{\partial Q_1^{l+1-j}\partial Q_2^{j}}\sum_{s=1}^{\min(l+1-j,k_1)}\frac{(i\hbar)^{s-1}\langle(\delta\hat{p}_1)^{k_1-s}(\delta\hat{p}_2)^{k_2}(\delta\hat{q}_1)^{n_1+l+1-j-s}(\delta\hat{q}_2)^{n_2+j}\rangle}{s!(k_1-s)!(l+1-j-s)!}$$
$$-k_2!\sum_{l=0}^{\infty}\sum_{j=0}^{l}\frac{1}{(l-j)!}\frac{\partial^{l+1}V(Q_1,Q_2)}{\partial Q_1^{l-j}\partial Q_2^{j+1}}\sum_{s=1}^{\min(j+1,k_2)}\frac{(i\hbar)^{s-1}\langle(\delta\hat{p}_1)^{k_1}(\delta\hat{p}_2)^{k_2-s}(\delta\hat{q}_1)^{n_1+l-j}(\delta\hat{q}_2)^{n_2+j+1-s}\rangle}{s!(k_2-s)!(j+1-s)!}$$
$$-k_1!k_2!\sum_{l=0}^{\infty}\sum_{j=0}^{l}\frac{\partial^{l+2}V(Q_1,Q_2)}{\partial Q_1^{l+1-j}\partial Q_2^{j+1}}\sum_{s=1}^{\min(k_1,l+1-j)}\frac{1}{s!(k_1-s)!(l+1-j-s)!}$$
$$\times\sum_{r=1}^{\min(k_2,j+1)}\frac{(i\hbar)^{s+r-1}\langle(\delta\hat{p}_1)^{k_1-s}(\delta\hat{p}_2)^{k_2-r}(\delta\hat{q}_1)^{n_1+l+1-j-s}(\delta\hat{q}_2)^{n_2+j+1-r}\rangle}{r!(k_2-r)!(j+1-r)!}. \tag{37}$$

A similar equation can be found for $d/dt\langle(\delta\hat{q}_1)^{n_1}(\delta\hat{q}_2)^{n_2}(\delta\hat{p}_1)^{k_1}(\delta\hat{p}_2)^{k_2}\rangle$. We do not have an explicit formula for the symmetric two-dimensional quantum hierarchy. Instead, we have used Maple procedures to calculate the hierarchy and to place the operators in symmetric order. (Details of these rather lengthy Maple procedures may be obtained from the authors.)

The infinite hierarchy of equations is truncated by dropping all moments beyond some chosen maximum order. The number of equations increases rapidly as the order of the moments increases. For two degrees of freedom, the number of equations is 14, 34, 69, 125, 209, ... when the maximum order of the moments is 2, 3, 4, 5, 6, ...

III. APPLICATION TO THE HÉNON-HEILES POTENTIAL

The Hénon-Heiles potential [5] is a well studied system that has a rich phase space structure, containing both chaotic and regular regions. Its classical Hamiltonian is given by

$$H=\frac{1}{2}(p_1^2+p_2^2)+\frac{1}{2}(q_1^2+q_2^2)+q_1^2q_2-\frac{1}{3}q_2^3. \tag{38}$$

The quantum Hamiltonian is obtained by replacing q and p with the operators $\hat{q}$ and $\hat{p}$. The first few equations of the quantum moment hierarchy for the Hénon Heiles system are

$$\frac{d}{dt}Q_1=P_1, \quad \frac{d}{dt}Q_2=P_2, \tag{39}$$

$$\frac{d}{dt}P_1=-Q_1-2Q_1Q_2-2\langle(\delta\hat{q}_1)(\delta\hat{q}_2)\rangle, \tag{40}$$

$$\frac{d}{dt}P_2=-Q_2-Q_1^2+Q_2^2-\langle(\delta\hat{q}_1)^2\rangle+\langle(\delta\hat{q}_2)^2\rangle. \tag{41}$$

It is apparent from Eq. (40) that we need to know the time development of $\langle(\delta\hat{q}_1)(\delta\hat{q}_2)\rangle$, which is given by

$$\frac{d}{dt}\langle(\delta\hat{q}_1)(\delta\hat{q}_2)\rangle=\langle(\delta\hat{p}_1)(\delta\hat{q}_2)\rangle+\langle(\delta\hat{p}_2)(\delta\hat{q}_1)\rangle. \tag{42}$$

It is apparent from Eq. (41) that we will need

$$\frac{d}{dt}\langle(\delta\hat{q}_1)^2\rangle=2\langle\tfrac{1}{2}[(\delta\hat{p}_1),(\delta\hat{q}_1)]_+\rangle \tag{43}$$

and

$$\frac{d}{dt}\langle(\delta\hat{q}_2)^2\rangle=2\langle\tfrac{1}{2}[(\delta\hat{p}_2),(\delta\hat{q}_2)]_+\rangle. \tag{44}$$

From Eq. (42), it is clear that we will need

$$\frac{d}{dt}\langle(\delta\hat{p}_1)(\delta\hat{q}_2)\rangle=\langle(\delta\hat{p}_1)(\delta\hat{p}_2)\rangle-(1+2Q_2)\langle(\delta\hat{q}_1)(\delta\hat{q}_2)\rangle -2Q_1\langle(\delta\hat{q}_2)^2\rangle-2\langle(\delta\hat{q}_1)(\delta\hat{q}_2)^2\rangle, \tag{45}$$

$$\frac{d}{dt}\langle(\delta\hat{p}_2)(\delta\hat{q}_1)\rangle=\langle(\delta\hat{p}_1)(\delta\hat{p}_2)\rangle-2Q_1\langle(\delta\hat{q}_1)^2\rangle +(2Q_2-1)\langle(\delta\hat{q}_1)(\delta\hat{q}_2)\rangle-\langle(\delta\hat{q}_1)^3\rangle +\langle(\delta\hat{q}_1)(\delta\hat{q}_2)^2\rangle, \tag{46}$$

and from Eq. (43) we will need

$$\frac{d}{dt}\langle\tfrac{1}{2}[(\delta\hat{p}_1),(\delta\hat{q}_1)]_+\rangle=\langle(\delta\hat{p}_1)^2\rangle-(2Q_2+1)\langle(\delta\hat{q}_1)^2\rangle -2Q_1\langle(\delta\hat{q}_1)(\delta\hat{q}_2)\rangle -2\langle(\delta\hat{q}_1)^2(\delta\hat{q}_2)\rangle. \tag{47}$$

These first few equations illustrate the fact that each equation brings in higher order moments and the system does not terminate.

So far there has not been any appearance of $\hbar$ in the quantum equations. The first occurrence of $\hbar$ is in the expression for $d/dt\langle(\delta\hat{p}_2)^3\rangle$. Until that point, the classical and quantum hierarchies have the same form.

A. Initial state

For our initial state, we have chosen a minimum uncertainty wave packet centered at an arbitrary point in phase space, whose coordinates and momenta are distinguished by a subscript ''o'':

$$\psi(q_1,q_2)=\frac{1}{\sqrt{2\pi}a}\exp\left[-\frac{(q_1-q_{1o})^2}{4a^2}+\frac{ip_{1o}q_1}{\hbar} -\frac{(q_2-q_{2o})^2}{4a^2}+\frac{ip_{2o}q_2}{\hbar}\right]. \tag{48}$$

Here $a^2=\langle(\delta q)^2\rangle$ is the mean squared half-width of the position probability distribution for each degree of freedom. The initial values of the quantum moments are computed from this wave function. The initial values of the classical moments were first chosen to be equal to the initial quantum moments, but this choice will be reconsidered later, since some of the quantum moments take on classically impossible values.

B. Computational accuracy

The hierarchy of moment equations was truncated at various orders and solved numerically. Essentially the same results were obtained when the truncation was at fourth, fifth, or sixth order moments. But as the moments grow in magnitude, there comes a time when the system becomes unstable. This is signaled by various moments diverging to infinity, and even-order moments taking on physically impossible negative values. This happens when the width of the probability distribution is no longer small compared to the scale of the potential. We have tried reformulating the moment expansion in terms of cumulants, and truncating the cumulant expansion, but this did not improve the stability of the system. Evidently, no truncation of the moment hierarchy is valid outside of the regime of narrow wave packets (Ehrenfest regime). But within this regime, the method is very reliable.

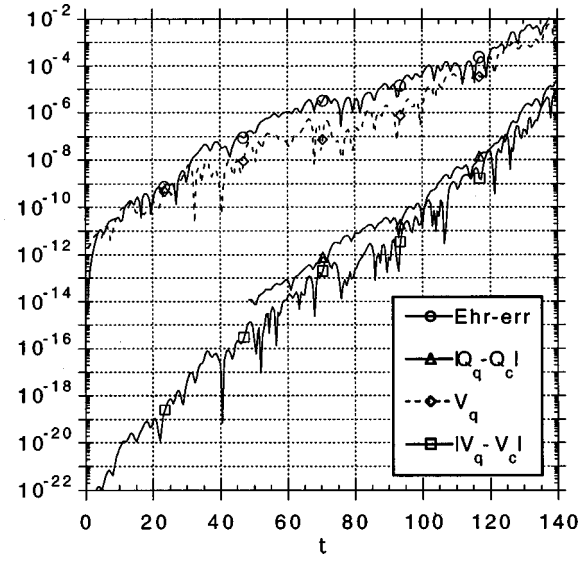

FIG. 1. Initial classical moments equal to quantum moments. Parameters for chaotic initial state: $q_{1o}=0$, $q_{2o}=-0.15$, $p_{1o}=0.474\,61$, $p_{2o}=0$. $a=10^{-6}$, $\hbar=2\times10^{-12}$. See text for definition of the curves.

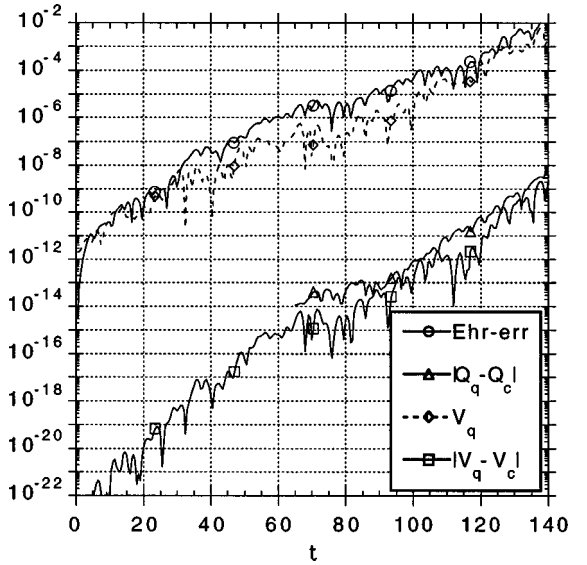

FIG. 2. Same as Fig. 1, except that the initial classical moments are derived from a Gaussian distribution.

The expectation value of the Hamiltonian should be a constant of motion, and the accuracy to which it is conserved is a check on the accuracy of the numerical computation. We found it to be accurately conserved to one part in 10^{10} in double precision until the distributions became too broad and the system became unstable.

C. Results

Most of the figures show four quantities as a function of time. ''Ehr-err,'' the error in applying Ehrenfest's theorem, is the distance between the centroid of the wave packet and the classical trajectory. ''$|Q_q-Q_c|$'' is the distance between the centroids of the quantum and classical probability distributions. In calculating both of these distances, the position coordinates q_1 and q_2 are regarded as the rectangular coordinates of a two-dimensional vector, and the magnitude of a vector difference is plotted as a suitable measure of the distance between two objects. The sum of the variances of the two coordinates,

$$V=\langle(\delta q_1)^2\rangle+\langle(\delta q_2)^2\rangle, \tag{49}$$

is taken as the measure of the spread of the probability distributions. We plot ''V_q'', the total variance of the quantum position distribution, and ''$|V_q-V_c|$'', the magnitude of the difference between the variances of the quantum and classical distributions.

The initial state for Figs. 1–6 is located in a region of phase space known to contain a chaotic trajectory, on a hypersurface of energy $E=0.125$. Because the moment expansion diverges and the equations of motion become unstable when the probability distribution becomes too broad, we halt the computation when the total variance V_q rises to approximately 10^{-2}.

The differences, $|Q_q-Q_c|$ and $|V_q-V_c|$, are much smaller than the quantities being subtracted, and so the results must be examined for numerical significance. Both Q_q and Q_c are of order unity, so their difference computed in double precision cannot be significant below 10^{-16}. In fact other computational errors limit the reliability of $|Q_q-Q_c|$ to computed values greater than about 10^{-14}, so the distance between the centroids is not plotted unless it exceeds this safe minimum. However, the difference between the variances, $|V_q-V_c|$, is no smaller than a factor of 10^{-10} below V_q, so the computed values of $|V_q-V_c|$ are reliable for the full range plotted in the figures.

Since the variance of the position distribution is the lowest order correction to Ehrenfest's theorem [see Eq. (10)], it is not surprising that the variance V_q and the Ehrenfest-theorem error exhibit a similar time dependence in Fig. 1. But it is much more appropriate to compare the quantum probability distribution with the classical distribution than to compare the centroid of the quantum distribution with a single classical trajectory. The distance between the centroids of the quantum and classical probability distributions, $|Q_q-Q_c|$, is much smaller than the distance between the centroid of the wave packet and a single classical trajectory.

In computing Fig. 1, the classical moments were given the same initial values as the quantum moments for the initial Gaussian state. But some of the values of the quantum moments are impossible for a classical probability distribution to realize. For example, the following quantum moment has a negative value:

$$\langle\tfrac{1}{2}[\delta\hat{p}_1\delta\hat{p}_2,\delta\hat{q}_1\delta\hat{q}_2]_+\rangle=-\frac{\hbar^2}{4}, \tag{50}$$

whereas the corresponding classical moment, $\langle\delta p_1\delta p_2\delta q_1\delta q_2\rangle$, has the value zero, because it is the average of the product of four independent Gaussian variables. The quantum moment $\langle(\delta\hat{p}_1)^2(\delta\hat{q}_2)^2\rangle$ has the value $\hbar^2/4$, the same as the corresponding classical moment. But the quantum moment $\frac{1}{2}\langle[(\delta\hat{p}_1)^2,(\delta\hat{q}_1)^2]_+\rangle$ has the negative value $-\hbar^2/4$, whereas the corresponding classical moment has the positive value $\hbar^2/4$. The differences between the

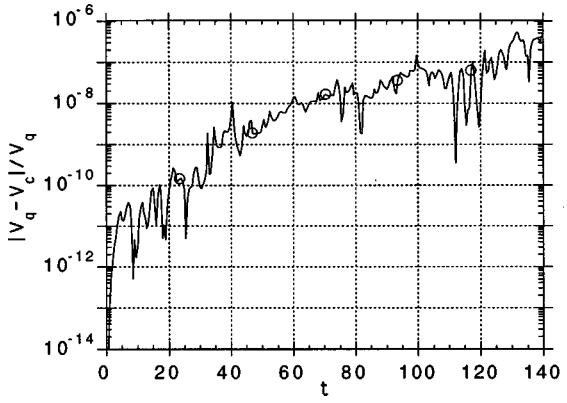

FIG. 3. Ratio of the difference between classical and quantum variances to the quantum variance, showing that the difference grows more rapidly than do the variances themselves.

classical and quantum moments are due to the noncommutation of the quantum operators.

For all calculations from Fig. 2 onwards, the initial classical moments were given values that correspond to independent Gaussian distributions of the position and momentum variables, having the same mean and variance as the quantum probability distributions. The results shown in Fig. 2 differ from Fig. 1 only through these changes in the initial classical data. Notice that the distance between the centroids of the classical and quantum distributions, $|Q_q - Q_c|$, and the difference between the variances of the two distributions, $|V_q - V_c|$, become *smaller* when this change is made to the classical initial data. Evidently, a better classical approximation to the quantum state is obtained if we use a physically realistic classical probability distribution, instead of trying to mimic those quantum moments whose values are classically impossible. It appears that the differences between the classical and quantum equations of motion are partly compensated by the differences between the classical and quantum initial data.

It is apparent in Fig. 2 that there are two time scales: the growth rate of ''Ehr-err'' and V_q, and that of $|Q_q - Q_c|$ and $|V_q - V_c|$. The former time scale is, as we shall argue, essentially classical, whereas the latter is a true measure of the difference between quantum and classical dynamics. The difference between the two scales is made explicit in Fig. 3, where the ratio $|V_q - V_c|/V_q$ is plotted.

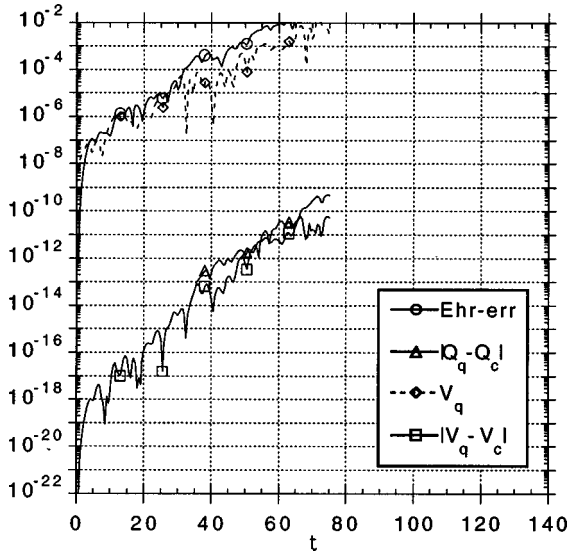

FIG. 5. Similar to Fig. 2, except that $\hbar = 2 \times 10^{-10}$.

The differences between the quantum and classical probability distributions are very much smaller than the quantities themselves, as can be seen from Fig. 2. To graphical accuracy, V_q cannot be distinguished from the classical variance V_c, and the distance between the classical trajectory and the centroid of the quantum probability distribution, labeled ''Ehr-err,'' cannot be distinguished from the distance between the trajectory and the centroid of the classical distribution. Thus, to a high degree of approximation, both ''Ehr-err'' and V_q grow at a rate determined by classical dynamics. The more rapid growth rate of the small differences between quantum and classical probability distributions is due to the $\hbar$ dependent terms that distinguish the quantum equations of motion from their classical counterparts.

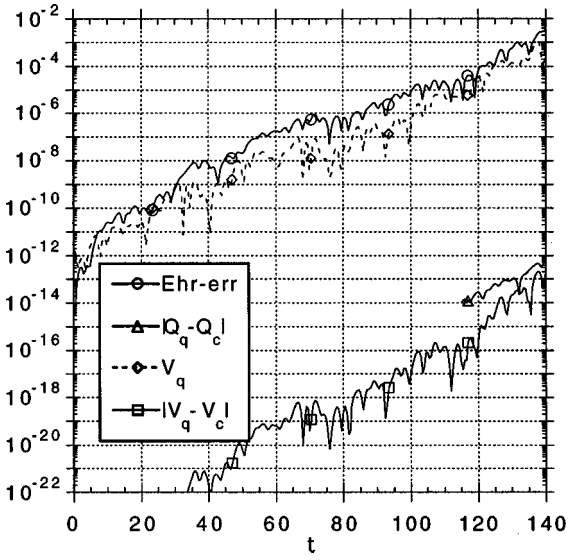

FIG. 4. Similar to Fig. 2, except that $\hbar = 2 \times 10^{-14}$.

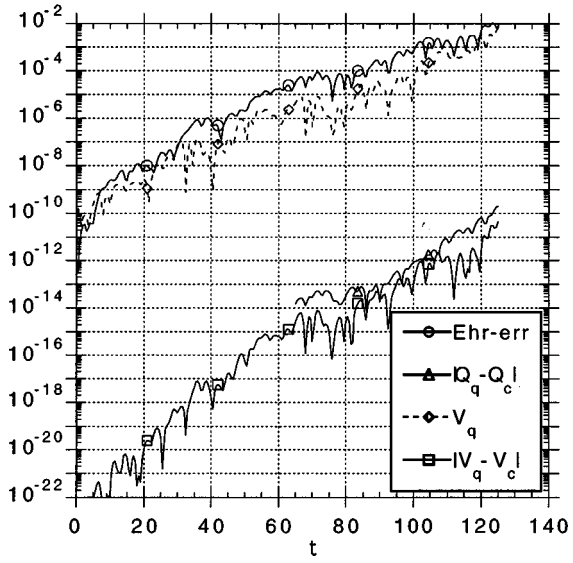

FIG. 6. Similar to Fig. 2, except that $a = 10^{-5}$.

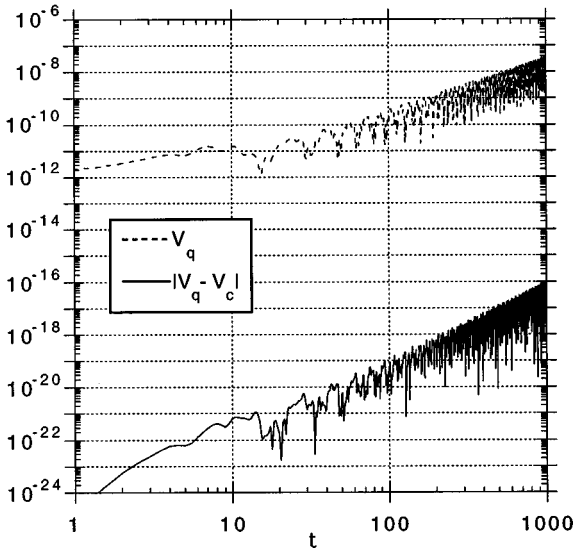

FIG. 7. Parameters for regular initial state: $q_{1o}=0$, $q_{2o}=0.20$, $p_{1o}=0.46\,404$, $p_{2o}=0$. $a=10^{-6}$, $\hbar=2\times10^{-12}$.

By varying the parameters $\hbar$ and a (the width of the initial state), we can distinguish truly quantum mechanical effects from effects due to the shape of the initial state. We shall see that the quantities ''Ehr-err'' and V_q depend mainly on the initial state, whereas the differences between the quantum and classical probability distributions, $|Q_q-Q_c|$ and $|V_q-V_c|$, scale as $\hbar^2$.

Figure 4 differs from Fig. 2 by reducing $\hbar$ by a factor of 10^{-2} but keeping a constant. The difference between the centroids of the quantum and classical distributions, $|Q_q-Q_c|$, and the difference between their variances, $|V_q-V_c|$, are reduced by a factor of 10^{-4}. However, ''Ehr-err'' and V_q change by only a small amount. As $\hbar$ is further reduced with a held constant, those two quantities are practically unchanged, while $|Q_q-Q_c|$ and $|V_q-V_c|$ continue to scale as $\hbar^2$.

When $\hbar$ is increased with a constant, in Fig. 5, $|Q_q-Q_c|$ and $|V_q-V_c|$ increase as $\hbar^2$. ''Ehr-err'' and V_q also increase, even though a is constant, because of the increased width of the momentum distribution, $\Delta p=\hbar/2a$. The greater velocity dispersion in the initial state is responsible for the larger values of the variance V_q, which in turn governs the growth of ''Ehr-err.''

In Fig. 6 we have increased a with $\hbar$ held constant. The differences $|Q_q-Q_c|$ and $|V_q-V_c|$ are essentially unchanged, while V_q and ''Ehr-err'' become larger. All these results together show that the true measures of the size of the quantum effects are the differences between the quantum and classical distributions, $|Q_q-Q_c|$ and $|V_q-V_c|$, which scale with $\hbar^2$. The difference between the quantum average and a single classical trajectory, ''Ehr-err,'' depends mainly on the shape of the initial state, and is not directly related to $\hbar$.

The initial state for Fig. 7 is located in a region of phase space that contains regular trajectories. The widths of the distributions and the various differences grow much more slowly in this case than in the chaotic case. The magnitude of the Ehrenfest-theorem error parallels the growth of the variance V_q; it is not plotted so as not to obscure the latter. The difference between centroids of the quantum and classical distributions, $|Q_q-Q_c|$, is so small that it cannot be calculated accurately in double precision, so it is not plotted. The difference $|Q_q-Q_c|$ can be made large enough to compute by making $\hbar$ sufficiently large, and by that means it has been verified that the evolution of $|Q_q-Q_c|$ closely parallels that of the difference between the variances, $|V_q-V_c|$.

Since the width of the classical distribution usually grows linearly in time for regular orbits, we expect the variances V_c and V_q to grow as t^2. This expectation is verified by the slope of the upper envelope of the curve of V_q vs t on the log-log plot. However, the upper envelope of the difference between the quantum and classical variances, $|V_q-V_c|$, grows as t^3.

IV. CONCLUSIONS

We have shown that a truncation of the moment hierarchy forms a useful method for studying the evolution of quantum and classical probability distributions, provided those distributions are sufficiently narrow. Within this regime Ehrenfest's theorem applies: the centroid of the quantum probability distribution approximately follows a classical trajectory. But, surprisingly, the error in Ehrenfest's theorem is not an essentially quantum effect. The deviation of the centroid of the probability distribution from a classical trajectory is governed by the variance of the probability distribution. Within the Ehrenfest regime, the classical and quantum variances are nearly equal, to several significant figures, so the error in applying Ehrenfest's theorem is effectively governed by classical quantities. In particular, it does not scale with $\hbar$, but rather is controlled by the width of the initial probability distribution.

A true measure of quantum effects is obtained by comparing quantum and classical probability distributions, i.e., by comparing the quantum state to an ensemble of classical trajectories. The difference between the centroids of the quantum and classical distributions, and between the variances of the two distributions, was found to scale as $\hbar^2$ and to be insensitive to the width of the initial state.

The differences between regular and chaotic motions can also be investigated by this method. For chaotic motions, the variances of the distributions grow exponentially, in analogy to the classical Lyapunov exponent. The difference between the centroids of the quantum and classical distributions, $|Q_q-Q_c|$, and the difference between the variances of the distributions, $|V_q-V_c|$, also grow exponentially, but with a larger exponent. In spite of their more rapid growth rate, the differences do not become comparable in magnitude to the quantities themselves. Before that happens the distributions become so wide that the moment expansion ceases to be valid, and the system enters a different dynamical regime.

For regular motions, the widths of the distributions grow linearly with time, and hence the variances grow as t^2. The differences between the quantum and classical centroids, and between the variances, grow more rapidly as t^3. Here also, the moment expansion breaks down before the differences become comparable to the quantities themselves.

These results allow us to resolve a problem that was posed by Joseph Ford (private communication). Chaotic classical mechanics has the attribute of *algorithmic complexity*, which is not possessed by quantum mechanics [6]. One

of the implications of this fact is that numerical errors grow exponentially in chaotic classical mechanics, and this limits the possibility of future prediction. Since numerical errors in quantum mechanics do not grow exponentially, someone might attempt to beat the prediction limit imposed by classical complexity by computing the path of a narrow quantum wave packet. Now such an attempt is almost certainly as misguided as attempting to build a heat engine that beats the second law of thermodynamics, but it is of interest to determine just why it must fail. Two possibilities suggest themselves. They are as follows.

(i) In a chaotic system the effect of a very small perturbation in the equation of motion can grow to dominate the solution. Perhaps the small differences between the quantum and classical equations (of order $\hbar^2$) can cause the path of the wave packet to diverge from the classical trajectory, so that the wave packet cannot be used to predict a chaotic classical trajectory.

(ii) The width of the wave packet grows exponentially (with approximately the classical Lyapunov exponent). When its width becomes comparable to the size of the system, the wave packet cannot predict even an approximate trajectory.

Our results show that it is (ii) that prevents quantum mechanics from circumventing the prediction limits of chaotic classical mechanics. Although the differences between quantum and classical dynamics grow more rapidly than the width of the probability distribution, they do not catch up to it before the width of the distribution becomes comparable to the size of the system.

ACKNOWLEDGMENTS

The authors are grateful for the financial support provided by the Natural Sciences and Engineering Research Council of Canada (NSERC). L.E.B. would like to acknowledge conversations with Joseph Ford, which motivated the study of this problem.

APPENDIX: COMMUTATOR IDENTITIES

This Appendix contains several commutator identities that are useful for deriving the quantum hierarchy of moment equations. Assume that we have two operators $\hat{A}$ and $\hat{B}$ that satisfy $[\hat{A},\hat{B}]=K\hat{I}$, where K is a constant and $\hat{I}$ is the identity operator. The commutator identity

$$[\hat{A}^j,\hat{B}^k]=\sum_{l=1}^{\min(j,k)}\frac{j!k!K^l}{l!(k-l)!(j-l)!}\hat{B}^{k-l}\hat{A}^{j-l} \tag{A1}$$

$$=-\sum_{l=1}^{\min(j,k)}\frac{j!k!(-K)^l}{l!(k-l)!(j-l)!}\hat{A}^{j-l}\hat{B}^{k-l} \tag{A2}$$

has been proved by Wilcox [7] and has been rediscovered at least once [8]. It is also useful to have a symmetric form of the above commutator identity,

$$[\hat{A}^j,\hat{B}^k]=-\sum_{l=1}^{\min([(j+1)/2],[(k+1)/2])}\frac{K^{2l-1}j!k!E_{2l-1}(0)}{(2l-1)!(k-2l+1)!(j-2l+1)!}[\hat{A}^{j-2l+1},\hat{B}^{k-2l+1}]_+, \tag{A3}$$

where $[x]$ indicates taking the integer part of x and $E_n(0)$ is the zeroth order coefficient of the nth Euler polynomial (see Abramowitz and Stegun [4], p. 809). The first few values of $E_n(0)$ are $E_0(0)=1$, $E_1(0)=-1/2$, $E_2(0)=0$, $E_3(0)=1/4$, $E_4(0)=0$, $E_5(0)=-1/2$, $E_6(0)=0$, $E_7(0)=17/8$, $E_8(0)=0$, and $E_9(0)=-31/2$. To prove this result, we can use Eq. (A1) to reorder $[\hat{A}^{j-2l+1},\hat{B}^{k-2l+1}]_+$ so that the $\hat{B}$'s are on the left and the $\hat{A}$'s are on the right. After some rearrangement, the right-hand side of Eq. (A3) becomes

$$-j!k!\sum_{l=1}^{\min(j,k)}\frac{K^l\hat{B}^{k-l}\hat{A}^{j-l}}{(k-l)!(j-l)!}\left[\frac{2E_l(0)}{l!}+\sum_{s=1}^{l-1}\frac{E_s(0)}{s!(l-s)!}\right], \tag{A4}$$

where we have used the fact that $E_{2n}(0)=0$. By converting $E_n(0)$ to Bernoulli numbers (B_n) using,

$$E_n(0)=-\frac{2}{(n+1)}(2^{n+1}-1)B_{n+1},\quad n=1,2,\ldots \tag{A5}$$

(see Abramowitz and Stegun [4], p. 805 23.1.20), and using the following properties:

$$\sum_{k=0}^{n-1}\frac{n!}{(n-k)!k!}B_k=0,\quad n\neq 1 \tag{A6}$$

(see Gradshteyn and Ryzhik [9], p. 1105 9.612),

$$B_n(x)=\sum_{k=0}^{n}\frac{n!}{k!(n-k)!}B_k x^{n-k} \tag{A7}$$

(see Gradshteyn and Ryzhik [9], p. 1106 9.620), $B_n(1/2)=-(1-2^{1-n})B_n$ (see Abramowitz and Stegun [4], p. 805 23.1.21), and $B_1=-1/2$, we can show that the quantity in square brackets in Eq. (A4) equals $-1/l!$, which completes the proof of Eq. (A3).

[1] L. E. Ballentine, Y. Yang, and J. P. Zibin, Phys. Rev. A **50**, 2854 (1994).
[2] M. Andrews and M. Hall, J. Phys. A **18**, 37 (1985).
[3] P. Ehrenfest, Z. Phys. **45**, 455 (1927).
[4] M. Abramowitz and I. A. Stegun, *Handbook of Mathematical Functions* (Dover Publications, New York, 1964).
[5] M. Hénon and C. Heiles, Astron. J. **69**, 73 (1964).
[6] J. Ford and G. Mantica, Am. J. Phys. **40**, 1086 (1992).
[7] R. M. Wilcox, J. Math. Phys. **8**, 962 (1967).
[8] R. Schack and A. Schenzle, Phys. Rev. A **41**, 3847 (1990).
[9] I. S. Gradshteyn and I. M. Ryzhik, in *Table of Integrals, Series, and Products*, 5th ed., edited by A. Jeffrey (Academic Press, New York, 1994).